Peer-reviewed version available at *Water* **2019**, *11*, 2559; doi:10.3390/w11122559

Article

What do plants leave after summer on the ground? – The effect of afforested plants in arid environments

César Dionisio Jiménez–Rodríguez [1,2]*, Miriam Coenders–Gerrits[1], Stefan Uhlenbrook[3], Jochen Wenninger [4]

[1] Department of Water Management, Water Resources Section, Delft University of Technology, 2600 GA, Delft, The Netherlands.
[2] Escuela de Ingeniería Forestal, Tecnológico de Costa Rica. P.O. Box 159-7050, Cartago, Costa Rica.
[3] UNESCO World Water Assessment Programme. Via dei Ceraioli, 45, 06134 Perugia PG, Italy.
[4] IHE Delft, Water Science and Engineering Department, 2611 AX, Delft, The Netherlands.
* Correspondence: cdjimenezcr@gmail.com

Abstract: Stable isotope concentrations in the soil, rain and ground water have been used to trace the water extraction zones of plants in different environments. The need to identify the plant water use by plants in afforestation programs to control desertification increases the importance of sap water partitioning of plants in sand dune areas. However, the introduction of new plant covers exerts pressure on the water resources and can affect the local soil water conditions. In this study, we analyzed the isotope concentrations in rain, soil, sap, and ground water after the summer of 2010. Two experimental plots established in the Hailiutu catchment (Shaanxi province, northwest China) were selected to gather the water samples between September and October 2010. One plot is dominated by Salix bushes (*Salix psammophila* C. Wang & Chang Y. Yang) and the other by the tree species Willow (*Salix matsudana* Koidz.). The total precipitation at the experimental site was 401 mm yr^{-1} during 2010, while 88.7 mm was collected in total for the period September to October. Willow trees transpired 12.82 kg d^{-1} being almost three times larger than Salix shrubs (4.57 kg d^{-1}). Despite the transpiration rates of both plant species and the few rain events in the region, the soil water beneath the plant covers is not depleted. Stable isotope signature of soil water beneath both covers shows the fractionation front in Salix at 20 cm depth and at Willow at 40 cm depth. However, soil water signature is closer to the groundwater than the collected rain water.

Keywords: stable water isotopes, deuterium, oxygen-18, soil water, fine root system

1. Introduction

Continental arid environments are characterized by excessive heat and variable precipitation distributed all over the year, with a tendency to a peak during summer months [1–3]. These conditions favoured the presence of a discontinuous vegetation cover characterized by banded and spotted shapes, large size variability, and specialized plant species [4,5]. The northern arid lands in China are an example of this type of environment, where the landscape is shaped by eolic erosion due to the high erodability of this soil type and the scarce ground cover protection [6–10]. Consequently, desertification in this region registered a strong growth of barren areas before 1999. However, after 2005 the plant cover experienced a positive change reducing the areas affected by desertification thanks to the rehabilitation and afforestation programs established in the region [11,12]. The current implementation of afforestation and agricultural programs modified the landscape cover with additional crop areas. These afforestation practices trigger a series of impacts to the environment due to the inadequate selection of plant species [13,14]. This increment in vegetation cover reduces the local surface temperature [15] and affects the local evaporation flux due to the increment of plant transpiration which depends mostly on groundwater [16–18].

Peer-reviewed version available at Water 2019, 11, 2559; doi:10.3390/w11122559

The evaporation (E) of arid environments is mainly composed of soil evaporation (E_s) and a small proportion of intercepted water by plant surfaces (E_i) and transpiration (E_t) [19–21]. The low precipitation rates underline the importance of soil water and groundwater availability for the plants. Rainfall interception decreases the water infiltration rates of vegetated areas in respect to bare soil conditions in arid and semi-arid regions [22,23]. This is the result of the quick evaporation of the intercepted water on the leaves, branches, and stem of the plants [19,21]. The relevance of interception increases considering the precipitation characteristics of the arid and semi–arid regions where the low volume, high intensity, lower and irregular frequency hinder the plant water acquisition [5]. Due to the scarce water resources in these regions the plants are adapted to quickly respond to environmental triggers such as the irregular rains. Thus increases the soil water acquisition by the plants and consequently its transpiration momentously [24,25].

The plant root system provides anchorage for the plant and an effective water extraction system [26]. This system absorbs the water close to the meristematic region of the root for its later use in the leaves [27–29]. Determination of water sources for the plants has been successfully done with the stable water isotopes oxygen-18 (δ^{18}O) and deuterium (δ^{2}H) [18,30–35]. The specific isotopic signatures of soil water is the result of a fractionation process that modifies the isotope composition[36], allowing to trace the water paths within the ecosystem [37]. The isotope signature of the absorbed water is not modified by plant uptake until the water reaches the photosynthetic tissues. Here, the leaf tissues will become enriched by the escape of lighter isotopes [38]. Althought the roots do not modify the soil water during uptake, the isotope signature of xylem water is affected by mixing processes when different water sources are used by the same plant. Analysis tools such as IsoSource [39] have been used in sand dunes bushes, corn and cotton plantations, woody species, and estuarine vegetation to determine the water sources of those covers [30–35]. Thus can provide information of the origin of water within the plant and if this water can be redistributed on the soil profile.

The increment of vegetated covers on arid environments exerts pressure on the scarce water resources. This has been the case with the introduction of Willow trees (*Salix matsudana*) and Salix bushes (*Salix psammophila*) in afforestation programs in the Hailiutu catchment [16–18]. The transpiration of these species increased the demand on the groundwater resource, however its influence on the soil water conditions are poorly understood. This work aims to describe the effect of Willow trees and Salix bushes on the soil water conditions after the summer. This will provide an indication of the vegetation influence on the soil water conditions beneath the covers.

2. Materials and Methods

2.1. Study Site

The study site is located within the Hailiutu catchment (area: 2645 km^2) in Yulin County; Shaanxi province; Northwest China (Figure 1). This catchment is part of the Maowusu semi-desert, which is characterized by undulating sand dunes over and dominated by a xeric scrubland. The nearest meteorological stations (Dong Shen: N 39.833° – E: 109.983°; Yanchi: N 37.800° – E 107.383°; and Yulin: N 38.233° – E: 109.700°) described a semi-arid continental climate with a mean annual precipitation of 386.1 mm yr^{-1} and a mean annual temperature of 8.6 °C (seasonal range: -17.4 °C to 27.1 °C). The soil type is classified as Calcaric Arenosols (ARc) with a high base saturation and a pH value over 8.0; with an excessive drainage due to its sandy texture [40]. The study site is composed of two experimental plots (see Appendix A1) located at 300 m from each other. The first plot is dominated by Salix bushes (*Salix psammophila* C. Wang & Chang Y. Yang) and has an area of 625 m^2 (2 5m x 2 5m). The second plot covers 81 m^2 (9 m x 9 m) and contains mainly individuals of Willow trees (*Salix matsudana* Koidz.) and Poplar trees (*Populus simonii* Carr.). In both plots soil water, groundwater, plant parameters, and soil

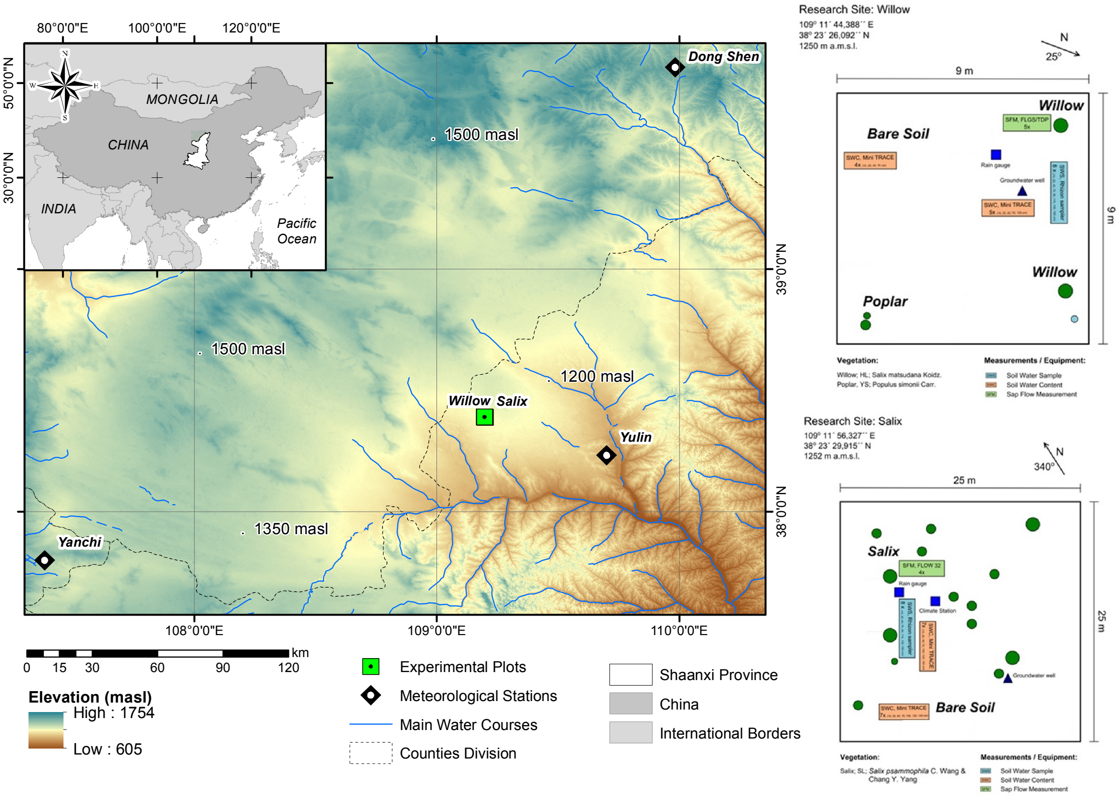

Figure 1. Geographical location of the experimental site (Willow–Salix) and the meteorological stations Dong Shen, Yanchi and Yulin used during the study period in the Shaanxi province, China. On the right hand side the experimental design of of both, Willow and Salix plots are shown.

variables were measured between September and October, 2010.

2.2. Hydrometric Data

Meteorological data was retrieved from the stations Dong Shen (1459 m.a.s.l.), Yanchi (1356 m.a.s.l.), and Yulin (1058 m.a.s.l.). The climatic data was downloaded from the National Oceanic and Atmospheric Administration (NOAA) [41]. This data set contains daily values of total precipitation (mm d^{-1}) and daily means for temperature (°C), dewpoint (°C), wind speed (m s^{-1}), and atmospheric pressure (mbar). Due the lack of solar radiation measurements in the selected study period; this variable was estimated according to Allen *et al.* [42] for missing data. Once all data was determined, the reference evaporation (E_o) was calculated with the FAO Penman–Monteith equation:

$$E_o = \frac{\Delta(R_n - G) + \rho_a C_p \frac{(e_s - e_a)}{r_a}}{\Delta + \gamma(1 + \frac{r_s}{r_a})} \tag{1}$$

where net radiation (R_n), soil heat flux (G), vapour pressure deficit of the air ($e_s - e_a$), Δ is the slope of the vapour-pressure relationship (kPa $°C^{-1}$), the psychrometric constant (γ), the air density (ρ_a) and the specific heat of the air (c_p) were used to determine the reference evaporation (E_o). The wind speed at 2 m height (u_2) was used to determine the aerodynamic resistance (r_a) and surface resistance (r_s). For daily time steps the soil heat flux is considered to equal 0 MJ $m^{-2} d^{-1}$ due the small daily differences [42].

Soil water measurements were carried out sporadically along the study period. The data collected corresponds to groundwater level (h, m) and soil moisture (θ, $\mathrm{m^3\,m^{-3}}$). The reference values of sandy soils for the permanent wilting point (θ_{WP}), field capacity (θ_{FC}) and saturation point (θ_{SP}) were $0.05\,\mathrm{m^3\,m^{-3}}$, $0.1\,\mathrm{m^3\,m^{-3}}$ and $0.46\,\mathrm{m^3\,m^{-3}}$, respectively [43]. The groundwater level was measured on a daily basis with one Mini-Diver (type: DI 501) in each plot. Soil water content was monitored with a Mini-TRASE sensor (type: 6050X3K1B) and the probes were located at 10 cm, 20 cm, 40 cm, 70 cm, and 100 cm depth beneath each species. On the Salix plot two more depths were monitored: 120 cm and 140 cm. The bare soil condition was monitored for both species at the same depths as Salix.

2.3. Water Sampling

Water samples were collected daily after each rain event to determine the isotopic signature of the precipitation, groundwater, soil water, and xylem water throughout the monitoring period. Soil water samples were taken with a Macro Rhizon (type: 4.5 mm Model) soil moisture sampler in both plots. The samples were collected at nine depths (10 cm, 20 cm, 40 cm, 70 cm, 90 cm, 110 cm, 140 cm, 150 cm and 160 cm), while the groundwater sampling depended on the water head elevation during the samplings. Xylem water was collected from an incision done at the twig of each tree; removing the bark, phloem, and cambium to prevent the collection of fractionated sap water. The incision location was far from the meristematic region, avoiding the fractionation linked to photosynthesis. Rain water was collected during the events to prevent fractionation by evaporation on an event basis. Each sample was sealed hermetically in 1.5 ml vials and transported to The Netherlands for their analysis. The isotopic composition was determined with a LGR Liquid Water Isotope Analyzer (type: DLT-100) with a precision of $< 0.3\,‰$ for $^{18}\mathrm{O}/^{16}\mathrm{O}$ and $< 1.0\,‰$ for $^{2}\mathrm{H}/^{1}\mathrm{H}$ and expressed in respect to the Vienna Standard Mean Ocean Water (VSMOW). The isotopic signature of each sample was expressed in respect to the VSMOW through the following equation [44]:

$$\delta = \left(\frac{R_{\mathrm{sample}}}{R_{\mathrm{standard}}} - 1\right) \tag{2}$$

where δ is the isotope composition of $^{18}\mathrm{O}$ and $^{2}\mathrm{H}$, R_{sample} and R_{standard} are the ratios of heavy to light isotopes ($^{18}\mathrm{O}/^{16}\mathrm{O}$ or $^{2}\mathrm{H}/^{1}\mathrm{H}$) of the sample and standard water, respectively.

2.4. Plant Parameters

For each plot the plant densities ($\mathrm{plants\,ha^{-1}}$), canopy heights (m), and leaf area index (LAI, $\mathrm{m^2\,m^{-2}}$) were measured to describe the stand conditions. Transpired water (E_{t}) was monitored in the Salix shrubs establishing four ring gauges (type: Dynagage Energy Balance sensor) in an individual of Salix; while five probes (type: Thermal Dissipation Probes) were installed in an individual of Willow. Each probe recorded the data at 10 minute intervals and those were summarized in an hourly and daily time step. Total mobilized water as transpiration was calculated with the product between the sapwood area and flow velocity. Sap wood area was measured through the average diameter of Salix twigs, and directly from a tree wood ring for the Willow tree. Wood ring area was obtained from inked water transported by capillary rise within the active sapwood sections, obtaining an area of $274.61\,\mathrm{cm^2}$ (A). Transpiration flow for each plant was obtained though the empirical equation developed by Granier [45]:

$$E_{\mathrm{t}} = 3600 \times 0.0119 \times \left(\frac{\partial T_{\mathrm{m}} - \partial T}{\partial T}\right) \times A \times \rho \tag{3}$$

where E_{t} is the transpiration ($\mathrm{g\,h^{-1}}$), ∂T is the temperature difference (°C), ∂T_{m} is the maximum temperature difference with zero E_{t} (°C), A is the cross section area ($\mathrm{cm^2}$), and ρ is the water density

Peer-reviewed version available at Water 2019, 11, 2559; doi:10.3390/w11122559

($\mathrm{g\,cm^{-3}}$).

The fine root system was described through the total root biomass (TRB, $\mathrm{kg\,m^{-3}}$) and the root length density (RLD, $\mathrm{cm\,cm^{-3}}$). The survey involved the collection of 80 samples of soil per species with an auger of $300\,\mathrm{cm^3}$ within a radius of 4.0 m. The sampling procedure was based on eight equidistant points from the stem towards the canopy edge, extracting 10 samples per point until a depth of 150 cm was reached. The samples were sieved to separate the soil from the roots, photographed on a scaled paper, and dried up following the procedure proposed by Cornelissen *et al.* [46] to determine the root length density (RLD, $\mathrm{cm\,cm^{-3}}$). The total root biomass was determined by weighing the dry cleaned roots with a digital balance. The total root length (cm) was determined by processing the root images with the use of the GIS free source software (www.gvsig.org). The total root length density was obtained dividing the total root length (cm) by the core volumes ($\mathrm{cm^3}$) [47].

2.5. Data Analysis

Plant differences were determined using an Analysis of Variance (ANOVA) with a $\mathrm{p_{value}}$ of 0.05. Statistical differences were determined with a Tukey HSD analysis. The plant water source of transpiration was determined using the software IsoSource [39].

3. Results

Total precipitation in 2010 was $401.0\,\mathrm{mm\,yr^{-1}}$ at the experimental site, registering a slightly wet condition in respect to the regional average of $386.1\,\mathrm{mm\,yr^{-1}}$. However, the precipitation was not enough to supply the yearly E_o at the site ($1339.1\,\mathrm{mm\ yr^{-1}}$) which is driven by the erratic relative humidity and small amount of precipitation all over the year (Figure 2). The $938.1\,\mathrm{mm\,yr^{-1}}$ difference between precipitation and reference evaporation support the Arid Steppe classification due to its annual water deficit [3,5,48,49]. September and October 2010 experienced $48.2\,\mathrm{mm\,month^{-1}}$ and $40.5\,\mathrm{mm\,month^{-1}}$ accounting for 12.0% and 10.1% of the annual precipitation, respectively. The water availability experienced during the study period allowed the presence of soil moisture above the permanent wilting point (θ_{WP}) for sandy soils ($0.05\,\mathrm{m^3\,m^{-3}}$) while the field capacity (θ_{FC}) was exceeded only in the deepest layers in both plots (Figure 3). Additionally, soil moisture increases with depth in Salix and Willow stands, keeping higher values than under bare soil conditions.

Hourly transpiration differs in amount and timing between species. Figure 4 shows the differences along five days where the sap flux for Willow is remarkably higher than Salix. Willow shows a larger capacity to transpire water with peak fluxes averaging $1549.1\,\mathrm{g\,hr^{-1}}$; whereas Salix peaks do not exceed $500\,\mathrm{g\,hr^{-1}}$ on average. Daily transpiration rates in both species depict a significant decreasing trend (ANCOVA, F= 36.09; n= 87, p= 0.0000) and a statistical difference between total daily rates (ANCOVA, F= 63.05, n=87, p= 0.0000), where Salix transport an average of $4.57\,\mathrm{kg\,d^{-1}}$ being three times smaller than Willow fluxes ($12.82\,\mathrm{kg\,d^{-1}}$). In addition, as transpiration is a physiological response to environmental climatic parameters the correlation analysis ($p < 0.001$) shows a significant positive correlation with temperature (0.47) and net radiation (0.35); while wind speed (0.05) and relative humidity (-0.27) are not significant.

Rain during the study period has a wide range of isotope signatures (see Appendix A2). The evaporation front in both stands is identifiable at 40 cm depth for both isotopes (Figure 5). The isotope signature of deep water samples lie close to the rain water signature, depicting the effect of local groundwater recharge having a similar signature to local rains. However, the soil above 10 cm depth depicts a wide range in their signatures. Sap water signature in both species seems to contain fractionated and non-fractionated water. Soil water contribution to xylem water from deep soil layers

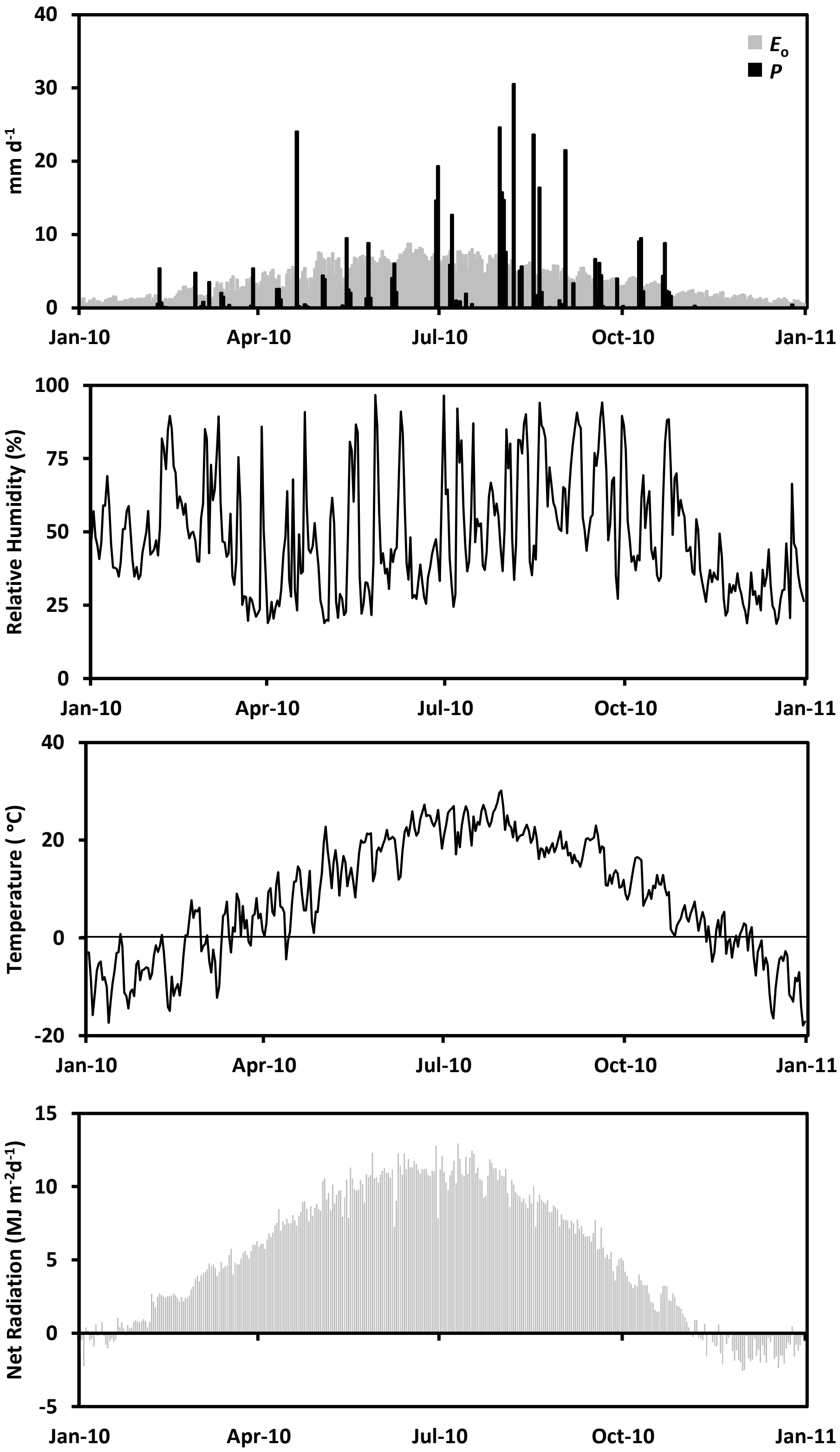

Figure 2. Meteorological conditions registered during 2010 at the research site based on the data of Dong Shen, Yanchi and Yulin meteorological stations

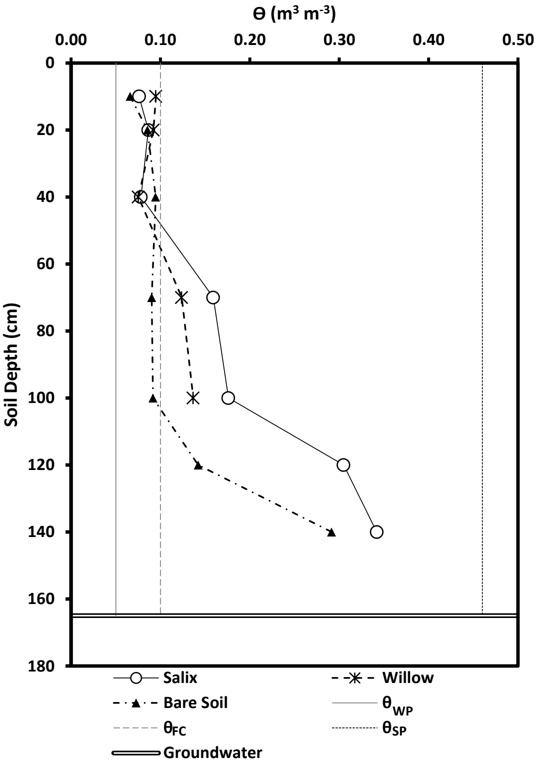

Figure 3. Soil moisture ($m^3\ m^{-3}$) measured in both plots for Salix, Willow and bare soil conditions during the study period

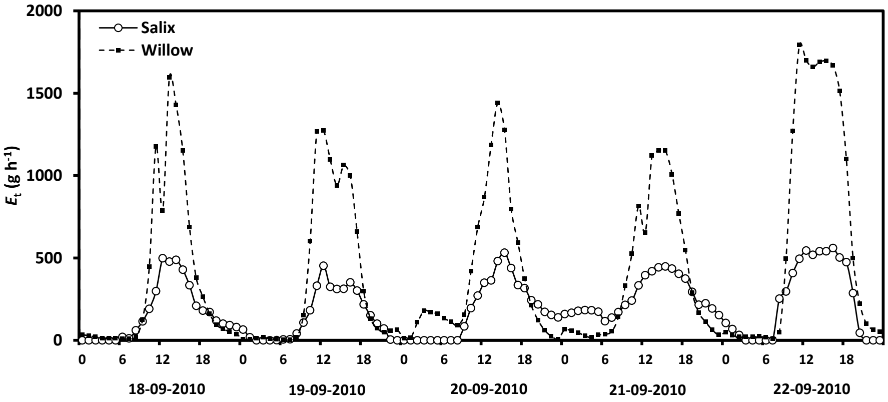

Figure 4. Hourly transpiration flow measured in Willow and Salix plants during the study period

Peer-reviewed version available at *Water* **2019**, *11*, 2559; doi:10.3390/w11122559

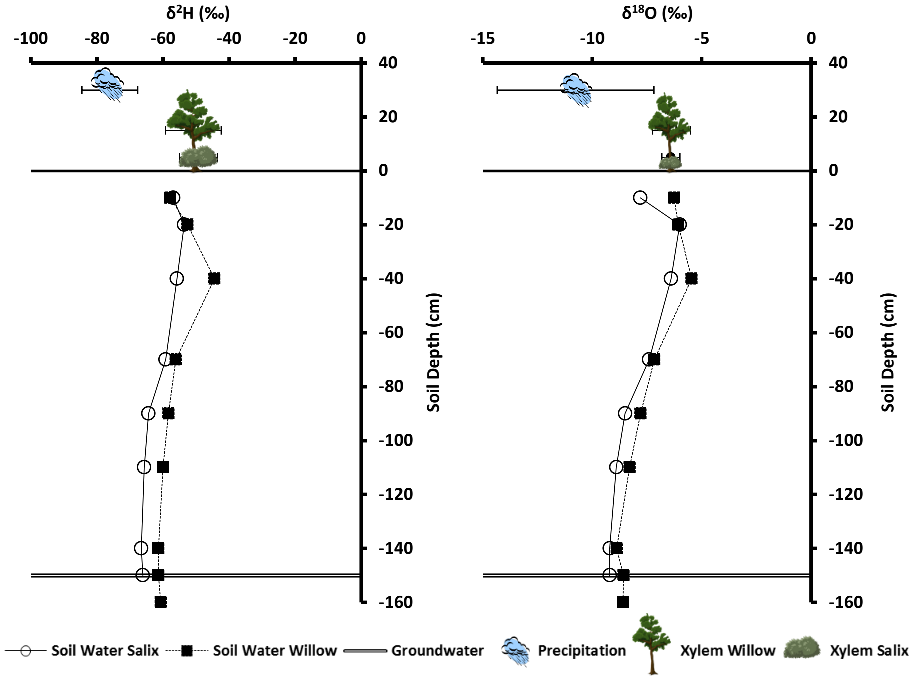

Figure 5. Evaporation front beneath Willow and Salix stand for oxygen-18 and deuterium water isotope signatures at the experimental site during autumn. The width of the canopy of each species in the graph corresponds to the standard deviation of the xylem water samples collected.

show a similar proportion in both species. Preliminary, only the 40 cm and 10 cm soil layers provides a strong contribution in Willow and Salix respectively. Therefore "a posteriori aggregation" [39] was performed, grouping the soil layers according to their similarities between isotopic signatures, evaporation front presence, and proximity within the soil profile. The grouping was settled as: 0-30 cm, 30-60 cm, >60 cm; including in the last soil layer the groundwater due its isotopic similarity with the deeper soil waters. The IsoSource output shows all the possible solutions to match the sap water mixture of δ^2H and δ^{18}O (Figure 6). The Willow stand shows a well-defined proportion of soil water contributions among the three water sources. The deep water source (>60 cm) contributes with a proportion lower than 0.08 to the sap water mixture, while the upper soil layers (<30 cm) provides between 0.28 and 0.48 of the mixed water, and the intermediate soil layers (30-60 cm) own the higher contribution values from 0.50 to 0.64. The clear differentiation between soil water sources in Willow is not visible for Salix. This species shows overlapping contributions of the water sources mainly for the superficial soil layers (0-60 cm), showing the deepest water source a contribution ranging from 0.21 to 0.54 (Figure 6).

Plant densities differ between stands, where the Salix stand has the higher plant density (900 trees ha^{-1}) with an average height of 2.6 ± 0.6 m. In contrast, the Willow stand has a plant density three times smaller (300 trees ha^{-1}) but with higher trees (3.5 ± 0.5 m). However, the LAI is affected by the leaf size and canopy diameter of the individual plants, where Salix register a leaf area index of 0.39 $\text{m}^2\,\text{m}^{-2}$ which is twice smaller than Willow (0.68 $\text{m}^2\,\text{m}^{-2}$). Underground stand characteristics also differ between species. Willow trees fix a larger root biomass beneath the 45 cm depth than Salix shrubs. Moreover, the root length density distribution shows a bimodal accumulation in Salix: at the soil surface (0-30 cm) and at mid depth (55-70 cm). Oppositely, Willow has three sections with high RLD values. The first two sections follow the Salix pattern, with an additional accumulation bellow 105 cm. The fine root distribution in both species expressed as RLD, provide them a good system for soil water acquisition for the superficial soil layers (Figure 6).

Peer-reviewed version available at *Water* **2019**, *11*, 2559; doi:10.3390/w11122559

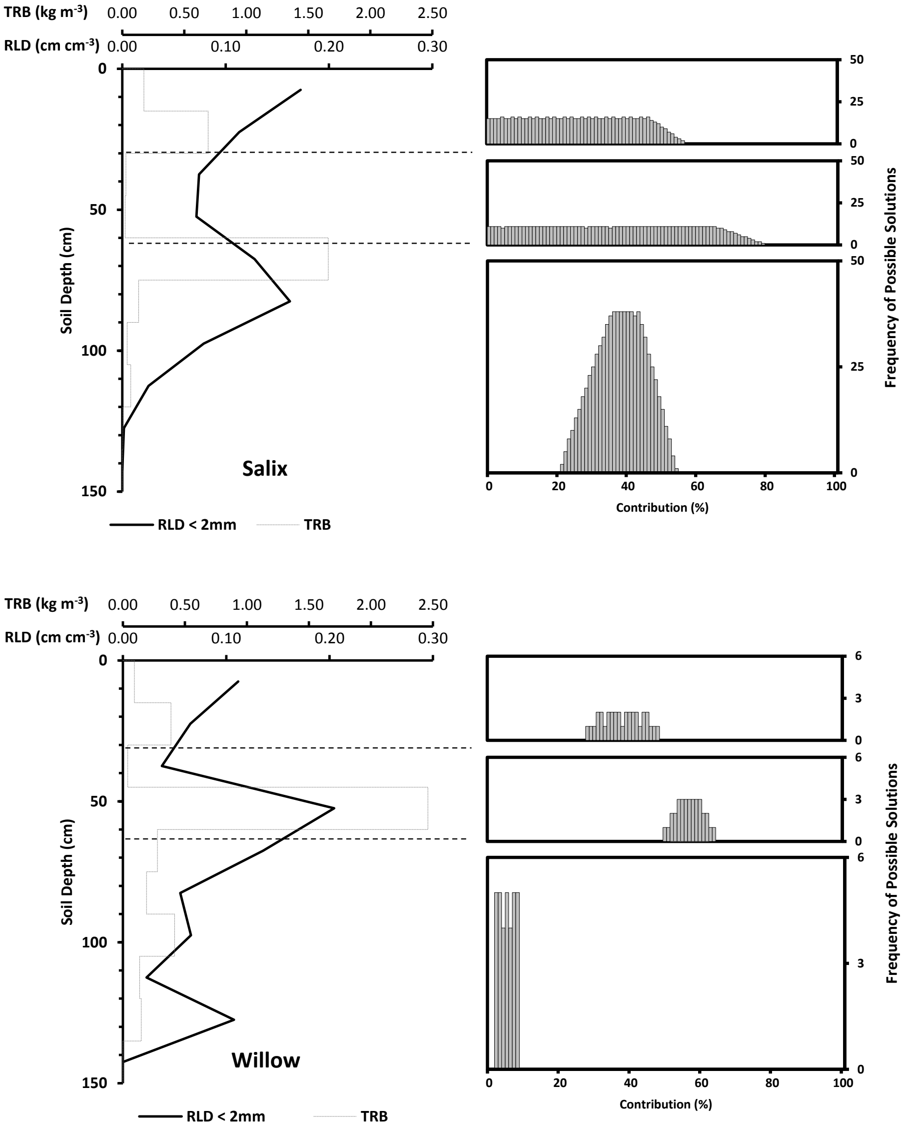

Figure 6. Root length density and total root biomass distribution along the soil profile, and its relation with the IsoSource distributions for all possible solutions to match the sap water mixture of Willow and Salix based on δ^2H and δ^{18}O isotope signatures.

Peer-reviewed version available at Water 2019, 11, 2559; doi:10.3390/w11122559

4. Discussion

The isotopic values of groundwater are similar to local rain water, depicting a local groundwater recharge documented for the Hailiutu catchment [18]. This is the consequence of the high capacity to infiltrate water by the sandy soils [21]. Consequently, infiltrated water will be available for longer periods because soil water evaporation at soil depths between 10–30 cm can take several weeks [50]. The shallow groundwater recharge occurred during the previous growing season due to the high rainfall intensities ($> 5\,\mathrm{mm\,d^{-1}}$) between July and September. This phenomena has also been documented by Li *et al.* [51] in Taihang (China), reporting a daily groundwater recharge with rains ranging from $3.2\,\mathrm{mm\,d^{-1}}$ to $3.8\,\mathrm{mm\,d^{-1}}$. This recharge capacity has been registered in the provinces of Shangxi and Inner Mongolia, gattering from 9% to 12% of the long term annual precipitation [22].

Conversely to groundwater, the isotopic composition of the soil water in the unsaturated zone is affected by the interaction between vegetation cover and soil evaporation. Soil evaporation affects the isotopic signature of soil water in the unsaturated zone providing particular signatures at different soil layers [52–55]. Meanwhile the plant cover type reduces the soil evaporation, where lower θ in the top soil layer (0-10 cm) were registered for Salix shrubs in comparison to Willow trees. Conversely, the high θ under Salix in respect to Willow reflects the higher infiltration capacity of a low plant cover and total root biomass fixed.

However, the signature beneath the plant cover differs considerably. Willow illustrates the typical theoretical pattern of the evaporation front, while soil water isotopes beneath Salix do not clearly have this distribution. Beneath Willow trees, both isotopes depict the theoretical evaporation front, while beneath Salix it is visible only for δ^{18}O. This effect is responsible of the presence of the evaporation front generating the later heavy isotope enrichment in superficial soil layers [51,52,56–58] (see Figure 5).

The main differences in plant size, fine root distribution, and water uptake capacity between Willow and Salix underline the importance of selecting plant species with low water requirements in respect to their biomass for afforestation programs. Willow is capable to withdraw up to $12.8\,\mathrm{kg\,d^{-1}}$ of water, extracting more than 90% from soil layers above 60 cm depth. This species is capable to make use of the superficial soil water during the fall period, even if the groundwater level is shallow. Conversely, Salix shrubs show lower transpiration rates not higher than $5.0\,\mathrm{kg\,d^{-1}}$ extracted uniformly from the whole soil profile including the groundwater. This extraction pattern shown by Salix depicts a more efficient root system acquiring water from different soil water sources due their fine root distribution. During this period, both species extract more than 50% of the water from the upper soil layers, taking advantage of the sporadic autumn rains and residual soil water content. These results are congruent with the behavior of Salix during the growing season (May-July), where Salix uses water from both sources: soil and groundwater [18]. On the other hand, the soil water dependency during fall of Willow trees differ in their summer behavior as documented by Yin *et al.* [17]. During summer, Willow trees have access to soil and groundwater to maintain their water consumption.

Lower evaporation rates during the study period depict a lower water need for both species, that is visible in the diminution of sap flow rates. This water need reduction affects the water uptake of Willow, which registered a lower contribution of deep soil water sources while the water uptake by superficial roots is more constant. On the other hand, Salix shows a high dynamic root system which extracts water from all the available sources indifferently from the upper soil layers and a strong contribution of the deep sources. This contribution is linked to the root distribution, keeping a high root length density in comparison to the Willow tree. The groundwater dependency of Salix [18] implies a permanent deep water extraction during summer and fall, extracting more deep water than Willow trees during the fall season.

Peer-reviewed version available at *Water* **2019**, *11*, 2559; doi:10.3390/w11122559

Shallow groundwater levels prevent desiccation processes in scarce rainfall environments, providing a vast water source for adapted plants that use the water economically [59]. Even if both species do not differ in the root amount; their vertical distribution shows different root spots. Salix root distribution displays two zones, supporting the hierarchy theory proposed by [60]. The Salix can withdraw water from rains as stemflow, while the deeper roots can obtained from a constant source (groundwater in this case). The fine root distribution beneath the Willow exemplifies woody patches capacity to use rain water in a short time response [56], as well as the hierarchy theory of Schwinning and Sala [60]. The fine root distribution of Willow with three dense regions with RLD higher than $0.1\,\mathrm{cm\,cm^{-3}}$ allow them to use different soil water source depending on soil water availability.

Despite the few rains, water used of both plant species do not deplete the soil water on the soil layers above 100 cm. This can be linked to the presence of hydraulic lift, where the root system prevents the soil water depletion on upper soil layers thanks to the redistribution of deeper soil water (in this case, groundwater). The hydraulic lift allows the formation of water pools along the soil profile in water scarce environments [61,62]. This process requires the movement of soil water by the potential difference between roots and the soil [61–64], allowing the diffusion of water through the roots cell membranes. The hydraulic lift had been identified in different plant species such as *Prosopis tamarugo*, *Artemisia tridentata*, *Acer saccharum* and *Madicago sativa* [61].

The hydraulic lifted water has an isotope signature close to the groundwater. It is relocated during night periods and once it is on the superficial soil layers evaporation will happen affecting the isotope signature of soil water. This water relocation is maintained by Willow trees, which despite the larger transpiration rates the soil water is not shortened. Liste and White [62] mention a Willow as a tree with the water redistribution capacity, providing evidence related to the potential of Willow to use groundwater through this process. Other tree species such as *Eucalyptus kochii* has the capacity to redistribute groundwater [63], or use it as an strategy of competition in saline conditions like *Juniperus phoenicea* and *Pistacia lentiscus* [65].

5. Conclusions

Local rain events have the capacity to reach the shallow groundwater table due the high infiltration capacity of the sandy soils, while the remaining soil water in the non-saturated zone is affected by the evaporation depending on the plant cover characteristics. Differences on the isotope water concentration of sap water among species and soil depth allows the differentiation of three water sources for the plants. The water use by Salix does not show a strong differentiation among water sources. This species is capable of extract soil and ground water with different proportions according to water availability. On the other hand, Willow trees are able to extract soil water and groundwater with specific proportions. This capacity is linked to the root distribution along the soil profile. Despite the species preferences to withdraw water, during the study period both Salix and Willow extract more than the 50% of the daily water from the upper soil layers. Thus depicts the capacity of these plant species of make use of the sporadic autumnal rain events in the sandy areas of northern China and their capacity to relocate groundwater along the soil profile during the non rainy periods. The presence of both plants species (Willow and Salix) reduces the effect of soil evaporation, allowing the presence of a higher soil water content than under bare soil conditions. This augment in soil water can be linked to water redistribution thanks to the presence of fine roots along the soil profile and hydraulic lift by the plants.

Author Contributions: Project administration, J.W.; conceptualization, J.W. and S.U.; methodology, J.W., S.U. and C.J.R.; formal analysis, C.J.R., M.C.G. and J.W.; isotope measurements, J.W. and C.J.R.; data curation, C.J.R.;

Peer-reviewed version available at *Water* **2019**, *11*, 2559; doi:10.3390/w11122559

writing—original draft preparation, C.J.R. with inputs from all co-authors; writing—review and editing, C.J.R. with inputs from all co-authors; funding acquisition, J.W., S.U., M.C.G. and C.J.R.

Funding: This study was supported by the Dutch government's Asia Facility for China project Partnership for education and research in water and ecosystem interactions, the Groundwater Circulation and Rational Development in the Ordos Plateau project (1212010634204), Groundwater monitoring in the Ordos Basin, the National Natural Sciences Foundation of China (4103752), Shaanxi Science and Technology Research and Development Program (2011KJXX56), Honor Power Foundation. We also received support from Ministerio de Ciencia, Tecnología y Telecomunicaciones (PINN-MICITT, contract: PED-032-2015-1) and The Netherlands Organization for Scientific Research (NWO, grant: 863.15.022).

Acknowledgments: Special thanks to NUFFIC program through a NFP-Fellowship. Also, to L. Yin and J. Huang by their collaboration in the field.

Conflicts of Interest: The authors declare no conflict of interest.

Appendix A

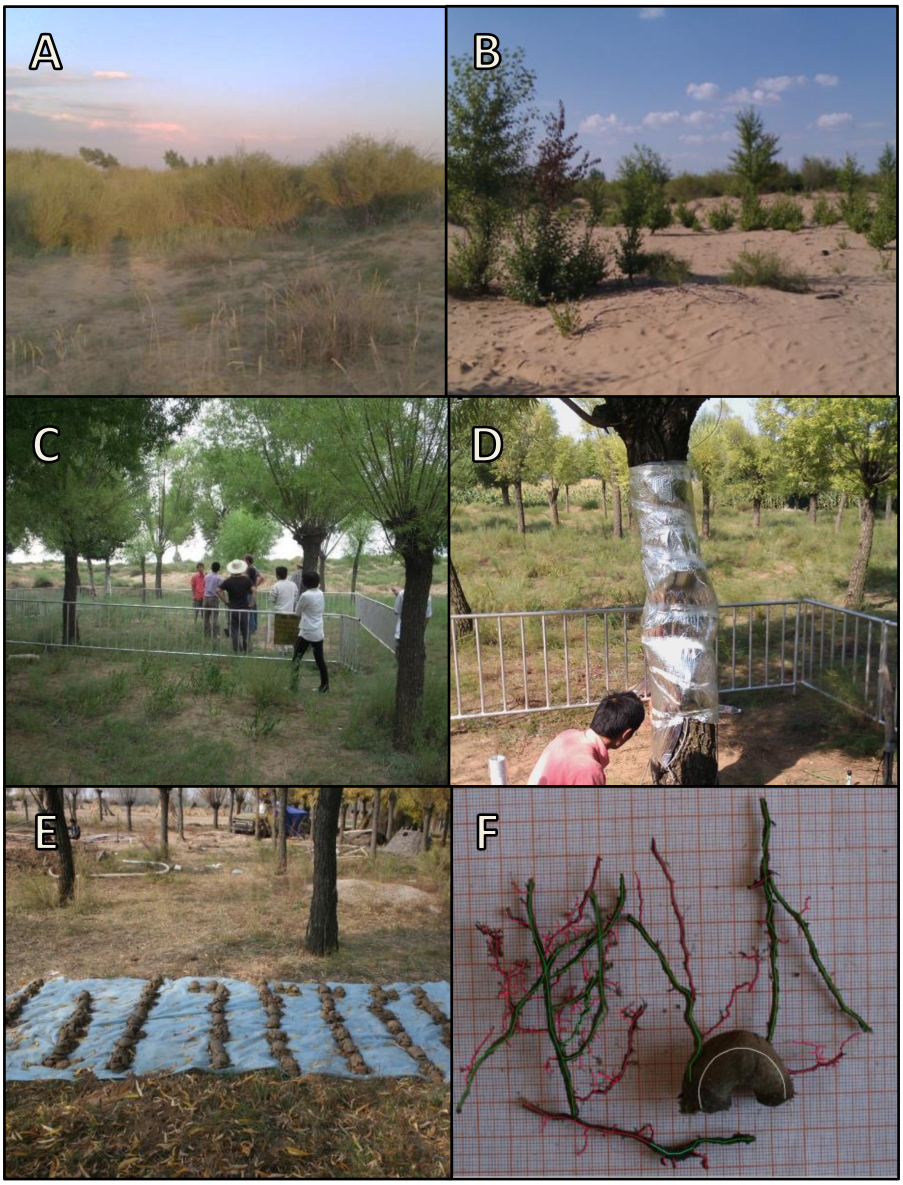

Figure A1. Photographs of the experimental sites and different sampling procedures carried out in Yulin County; Shaanxi province – China. Picture A: panoramic view of the bush lands dominated by Salix plants. Picture B: bare soil conditions close to the experimental plots. Picture C: experimental plot with Willow trees. Picture D: Thermal dissipation probe installed in a Willow Tree. Picture E: Root sampling within Willow plot. Picture F: print screen of the fine root measuring procedure.

Appendix B

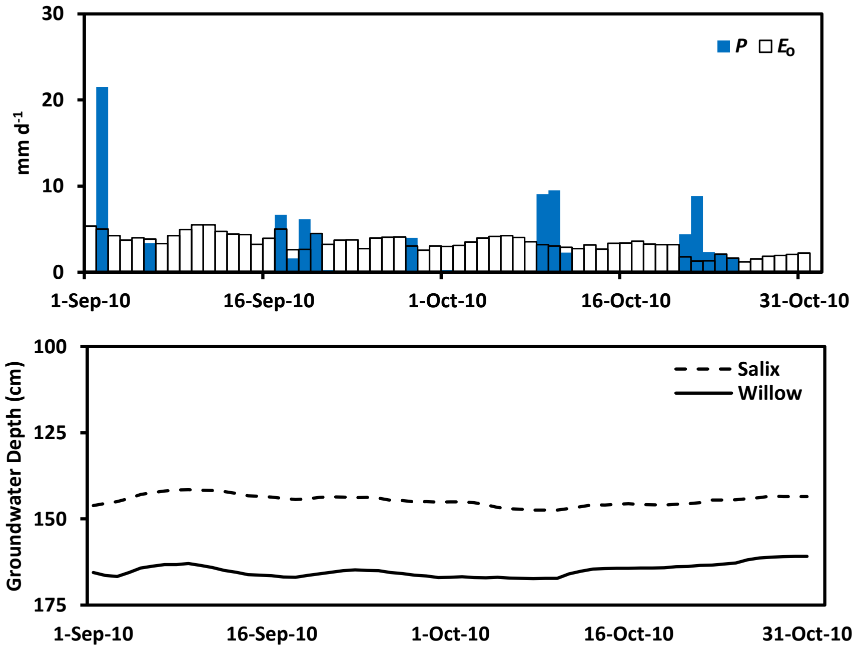

Figure A2. Daily measurements of precipitation, evaporation and groundwater depth during the monitoring period.

References

1. Abd El-Ghani, M.M.; Huerta-Martínez, F.M.; Hongyan, L.; Qureshi, R. Arid Deserts of the World: Origin, Distribution, and Features. In *Plant Responses to Hyperarid Desert Environments*; Springer International Publishing: Cham, 2017; pp. 1–7. doi:10.1007/978-3-319-59135-3_1.
2. Salem, B. *Arid zone forestry: a guide for field technicians.*; Number 20, Food and Agriculture Organization (FAO), 1989.
3. Bonan, G. *Ecological climatology: concepts and applications*; Cambridge University Press, 2002.
4. Aguiar, M.R.; Sala, O.E. Patch structure, dynamics and implications for the functioning of arid ecosystems. *Trends in Ecology Evolution* **1999**, *14*, 273 – 277. doi:10.1016/S0169-5347(99)01612-2.
5. Wainwright, J.; Mulligan, M.; Thornes, J. Plants and water in drylands. In *Eco-Hydrology: Plants and Water in Terrestrial and Aquatic Environments*; Baird, A.; Wilby, R., Eds.; Routledge, 1999; pp. 78–126.
6. FAO. *Guidelines for Soil Description.*; Food and Agriculture Organization (FAO), 2006.
7. Huggett, R. *Fundamentals of geomorphology*, second ed.; Routledge Fundamentals of Physical Geography, 2007.
8. Summerfield, M. *Global Geomorphology*; Longman, 1991.
9. Yang, X.; Zhang, K.; Jia, b.; Ci, L. Desertification assessment in China: An overview. *Journal of Arid Environments* **2005**, *63*, 517–531. doi:10.1016/j.jaridenv.2005.03.032.
10. Young, A. *Agroforestry for soil conservation*; CAB International, 1989.
11. Han, K.S.; Park, Y.Y.; Yeom, J.M. Detection of change in vegetation in the surrounding Desert areas of Northwest China and Mongolia with multi-temporal satellite images. *Asia-Pacific Journal of Atmospheric Sciences* **2015**, *51*, 173–181. doi:10.1007/s13143-015-0068-3.
12. Song, X.; Wang, T.; Xue, X.; Yan, C.; Li, S. Monitoring and analysis of aeolian desertification dynamics from 1975 to 2010 in the Heihe River Basin, northwestern China. *Environmental Earth Sciences* **2015**, *74*, 3123–3133. doi:10.1007/s12665-015-4350-6.
13. Cao, S.; Tian, T.; Chen, L.; Dong, X.; Yu, X.; Wang, G. Damage Caused to the Environment by Reforestation Policies in Arid and Semi-Arid Areas of China. *AMBIO* **2010**, *39*, 279–283. doi:10.1007/s13280-010-0038-z.

Peer-reviewed version available at *Water* **2019**, *11*, 2559; doi:10.3390/w11122559

14. Cao, S.; Chen, L.; Shankman, D.; Wang, C.; Wang, X.; Zhang, H. Excessive reliance on afforestation in China's arid and semi-arid regions: Lessons in ecological restoration. *Earth-Science Reviews* **2011**, *104*, 240–245. doi:10.1016/j.earscirev.2010.11.002.
15. Peng, S.S.; Piao, S.; Zeng, Z.; Ciais, P.; Zhou, L.; Li, L.Z.X.; Myneni, R.B.; Yin, Y.; Zeng, H. Afforestation in China cools local land surface temperature. *Proceedings of the National Academy of Sciences* **2014**, *111*, 2915–2919. doi:10.1073/pnas.1315126111.
16. Yang, Z.; Zhou, Y.; Wenninger, J.; Uhlenbrook, S. The causes of flow regime shifts in the semi-arid Hailiutu River, Northwest China. *Hydrology and Earth System Sciences* **2012**, *16*, 87–103. doi:10.5194/hess-16-87-2012.
17. Yin, L.; Zhou, Y.; Huang, J.; Wenninger, J.; Hou, G.; Zhang, E.; Wang, X.; Dong, J.; Zhang, J.; Uhlenbrook, S. Dynamics of willow tree (Salix matsudana) water use and its response to environmental factors in the semi-arid Hailiutu River catchment, Northwest China. *Environmental Earth Sciences* **2014**, *71*, 4997–5006. doi:10.1007/s12665-013-2891-0.
18. Zhou, Y.; Wenninger, J.; Yang, Z.; Yin, L.; Huang, J.; Hou, L.; Wang, X.; Zhang, D.; Uhlenbrook, S. Groundwaterndash;surface water interactions, vegetation dependencies and implications for water resources management in the semi-arid Hailiutu River catchment, China ndash; a synthesis. *Hydrology and Earth System Sciences* **2013**, *17*, 2435–2447. doi:10.5194/hess-17-2435-2013.
19. Roberts, J., Plants and water in forests and woodlands. In *Eco-Hydrology: Plants and Water in Terrestrial and Aquatic Environments*; Routledge, 1999; pp. 181–236.
20. Savenije, H.H.G. The importance of interception and why we should delete the term evapotranspiration from our vocabulary. *Hydrological Processes* **2004**, *18*, 1507–1511. doi:10.1002/hyp.5563.
21. Yaseef, N.R.; Yakir, D.; Rotenberg, E.; Schiller, G.; Cohen, S. Ecohydrology of a semi-arid forest: partitioning among water balance components and its implications for predicted precipitation changes. *Ecohydrology* **2009**, *3*, 143–154. doi:10.1002/eco.65.
22. Scanlon, B.R.; Keese, K.E.; Flint, A.L.; Flint, L.E.; Gaye, C.B.; Edmunds, W.M.; Simmers, I. Global synthesis of groundwater recharge in semiarid and arid regions. *Hydrological Processes* **2006**, *20*, 3335–3370. doi:10.1002/hyp.6335.
23. feng Zhang, Y.; ping Wang, X.; Hu, R.; xia Pan, Y.; Paradeloc, M. Rainfall partitioning into throughfall, stemflow and interception loss by two xerophytic shrubs within a rain-fed re-vegetated desert ecosystem, northwestern China. *Journal of Hydrology* **2015**, *527*, 1084–1095. doi:10.1016/j.jhydrol.2015.05.060.
24. Chesson, P.; Gebauer, R.L.E.; Schwinning, S.; Huntly, N.; Wiegand, K.; Ernest, M.S.K.; Sher, A.; Novoplansky, A.; Weltzin, J.F. Resource pulses, species interactions, and diversity maintenance in arid and semi-arid environments. *Oecologia* **2004**, *141*, 236–253. doi:10.1007/s00442-004-1551-1.
25. Ivans, S.; Hipps, L.; Leffler, A.J.; Ivans, C.Y. Response of Water Vapor and CO2 Fluxes in Semiarid Lands to Seasonal and Intermittent Precipitation Pulses. *Journal of Hydrometeorology* **2006**, *7*, 995–1010. doi:10.1175/JHM545.1.
26. Ogle, K.; Wolpert, R.L.; Reynolds, J.F. RECONSTRUCTING PLANT ROOT AREA AND WATER UPTAKE PROFILES. *Ecology* **2004**, *85*, 1967–1978. doi:10.1890/03-0346.
27. Cardon, Z.G.; Whitbeck, J.L. *The rhizosphere. An Ecological Perspective*; Elsevier Academic Press, Amsterdam, 2007.
28. Curl, E.; Truelove, B. The rhizosphere. Springer-Verlag, New York. *The rhizosphere. Springer-Verlag, New York.* **1986**.
29. Hopkins, W.G.; Hüner, N.P. *Introduction to Plant Physiology*; Wiley, 2008.
30. Jia, Z.; Zhu, Y.; Liu, L. Different Water Use Strategies of Juvenile and Adult *Caragana intermedia* Plantations in the Gonghe Basin, Tibet Plateau. *PLOS ONE* **2012**, *7*, 1–6. doi:10.1371/journal.pone.0045902.
31. Nie, Y.p.; Chen, H.s.; Wang, K.l.; Tan, W.; Deng, P.y.; Yang, J. Seasonal water use patterns of woody species growing on the continuous dolostone outcrops and nearby thin soils in subtropical China. *Plant and Soil* **2011**, *341*, 399–412. doi:10.1007/s11104-010-0653-2.
32. Rossatto, D.R.; da Silveira Lobo Sternberg, L.; Franco, A.C. The partitioning of water uptake between growth forms in a Neotropical savanna: do herbs exploit a third water source niche? *Plant Biology* **2012**, *15*, 84–92. doi:10.1111/j.1438-8677.2012.00618.x.
33. Swaffer, B.A.; Holland, K.L.; Doody, T.M.; Li, C.; Hutson, J. Water use strategies of two co-occurring tree species in a semi–arid karst environment. *Hydrological Processes* **2013**, *28*, 2003–2017. doi:10.1002/hyp.9739.

34. Wang, P.; Song, X.; Han, D.; Zhang, Y.; Liu, X. A study of root water uptake of crops indicated by hydrogen and oxygen stable isotopes: A case in Shanxi Province, China. *Agricultural Water Management* **2010**, *97*, 475–482. doi:10.1016/j.agwat.2009.11.008.
35. Wei, L.; Lockington, D.A.; Poh, S.C.; Gasparon, M.; Lovelock, C.E. Water use patterns of estuarine vegetation in a tidal creek system. *Oecologia* **2013**, *172*, 485–494. doi:10.1007/s00442-012-2495-5.
36. Geyh, M. Volume IV. Groundwater. Saturated and unsaturated zone. In *Environmental isotopes in the hydrological cycle: principles and applications*; Mook, W., Ed.; UNESCO, 2000.
37. Leibundgut, C.; Seibert, J. 2.09. Tracer Hydrology. In *Treatise on Water Science*; Wilderer, P., Ed.; Elsevier, 2011; pp. 215–236.
38. Butt, S.; Ali, M.; Fazil, M.; Latif, Z. Seasonal variations in the isotopic composition of leaf and stem water from an arid region of Southeast Asia. *Hydrological Sciences Journal* **2010**, *55*, 844–848. doi:10.1080/02626667.2010.487975.
39. Phillips, D.L.; Newsome, S.D.; Gregg, J.W. Combining sources in stable isotope mixing models: alternative methods. *Oecologia* **2005**, *144*, 520–527. doi:10.1007/s00442-004-1816-8.
40. IIASA/FAO. *Global Agro-Ecological Zones (GAEZ v3.0). IIASA, Laxenburg, Austria and FAO, Rome, Italy.*; 2012.
41. NCDC. NNDC Climate Data Online. http://www7.ncdc.noaa.gov/CDO/cdoselect.cmd, 2012.
42. Allen, R.G.; Pereira, L.S.; Raes, D.; Smith, M.; others. *Crop evapotranspiration-Guidelines for computing crop water requirements–FAO Irrigation and drainage paper 56*; 1998.
43. Saxton, K.E.; Rawls, W.J. Soil water characteristic estimates by texture and organic matter for hydrologic solutions. *Soil science society of America Journal* **2006**, *70*, 1569–1578. doi:10.2136/sssaj2005.0117.
44. Craig, H. Standard for Reporting Concentrations of Deuterium and Oxygen-18 in Natural Waters. *Science* **1961**, *133*, 1833–1834. doi:10.1126/science.133.3467.1833.
45. Granier, A. Une nouvelle méthode pour la mesure du flux de sève brute dans le tronc des arbres. *Annales des Sciences Forestières* **1985**, *42*, 193–200.
46. Cornelissen, J.; Lavorel, S.; Garnier, E.; Diaz, S.; Buchmann, N.; Gurvich, D.; Reich, P.; Ter Steege, H.; Morgan, H.; Van Der Heijden, M.; Pausas, J.; Poorter, H. A handbook of protocols for standardised and easy measurement of plant functional traits worldwide. *Australian journal of Botany* **2003**, *51*, 335–380. doi:10.1071/BT02124.
47. Huang, J.; Zhou, Y.; Yin, L.; Wenninger, J.; Zhang, J.; Hou, G.; Zhang, E.; Uhlenbrook, S. Climatic controls on sap flow dynamics and used water sources of Salix psammophila in a semi-arid environment in northwest China. *Environmental Earth Sciences* **2015**, *73*, 289–301. doi:10.1007/s12665-014-3505-1.
48. Kottek, M.; Grieser, J.; Beck, C.; Rudolf, B.; Rubel, F. World map of the Köppen-Geiger climate classification updated. *Meteorologische Zeitschrift* **2006**, *15*, 259–263. doi:10.1127/0941-2948/2006/0130.
49. Peel, M.C.; Finlayson, B.L.; Mcmahon, T.A. Updated world map of the Köppen-Geiger climate classification. *Hydrology and Earth System Sciences Discussions* **2007**, *4*, 439–473.
50. Noy-Meir, I. Desert Ecosystems: Environment and Producers. *Annual Review of Ecology and Systematics* **1973**, *4*, 25–51. doi:10.1146/annurev.es.04.110173.000325.
51. Li, F.; Song, X.; Tang, C.; Liu, C.; Yu, J.; Zhang, W. Tracing infiltration and recharge using stable isotope in Taihang Mt., North China. *Environmental Geology* **2007**, *53*, 687–696. doi:10.1007/s00254-007-0683-0.
52. Barnes, C.J.and Allison, G. Tracing of water movement in the unsaturated zone using stable isotopes of hydrogen and oxygen. *Journal of Hydrology* **1988**, *100*, 143–176. doi:10.1016/0022-1694(88)90184-9.
53. Brunel, J.P.; Walker, G.R.; Kennett-Smith, A.K. Field validation of isotopic procedures for determining sources of water used by plants in a semi-arid environment. *Journal of Hydrology* **1995**, *167*, 351–368. doi:10.1016/0022-1694(94)02575-V.
54. Rothfuss, Y.; Biron, P.; Braud, I.; Canale, L.; Durand, J.L.; Gaudet, J.P.; Richard, P.; Vauclin, M.; Bariac, T. Partitioning evapotranspiration fluxes into soil evaporation and plant transpiration using water stable isotopes under controlled conditions. *Hydrological Processes* **2010**, *24*, 3177–3194. doi:10.1002/hyp.7743.
55. Schwinning, S.; Ehleringer, J.R. Water use trade-offs and optimal adaptations to pulse-driven arid ecosystems. *Journal of Ecology* **2001**, *89*, 464–480. doi:10.1046/j.1365-2745.2001.00576.x.
56. Midwood, A.; Boutton, T.; Archer, S.; Watts, S. Water use by woody plants on contrasting soils in a savanna parkland: assessment with δ^2H and δ^{18}O. *Plant and Soil* **1998**, *205*, 13–24. doi:10.1023/A:1004355423241.

Peer-reviewed version available at *Water* **2019**, *11*, 2559; doi:10.3390/w11122559

57. Sutanto, S.J.; Wenninger, J.; Coenders-Gerrits, A.M.J.; Uhlenbrook, S. Partitioning of evaporation into transpiration, soil evaporation and interception: a comparison between isotope measurements and a HYDRUS-1D model. *Hydrology and Earth System Sciences* **2012**, *16*, 2605–2616. doi:10.5194/hess-16-2605-2012.
58. Wenninger, J.; Beza, D.T.; Uhlenbrook, S. Experimental investigations of water fluxes within the soil–vegetation–atmosphere system: Stable isotope mass-balance approach to partition evaporation and transpiration. *Physics and Chemistry of the Earth, Parts A/B/C* **2010**, *35*, 565–570. doi:10.1016/j.pce.2010.07.016.
59. Jiang, G.; He, W. Species- and habitat-variability of photosynthesis, transpiration and water use efficiency of different plant species in Maowusu Sand Area. *Acta Botanica Sinica* **1999**, *41*, 1114—1124.
60. Schwinning, S.; Sala, O.E. Hierarchy of responses to resource pulses in arid and semi-arid ecosystems. *Oecologia* **2004**, *141*, 211–220. doi:10.1007/s00442-004-1520-8.
61. Horton, J.L.; Hart, S.C. Hydraulic lift: a potentially important ecosystem process. *Trends in Ecology Evolution* **1998**, *13*, 232–235. doi:10.1016/S0169-5347(98)01328-7.
62. Liste, H.H.; White, J.C. Plant hydraulic lift of soil water – implications for crop production and land restoration. *Plant and Soil* **2008**, *313*, 1–17. doi:10.1007/s11104-008-9696-z.
63. Brooksbank, K.; White, D.A.; Veneklaas, E.J.; Carter, J.L. Hydraulic redistribution in Eucalyptus kochii subsp. borealis with variable access to fresh groundwater. *Trees* **2011**, *25*, 735–744. doi:10.1007/s00468-011-0551-0.
64. Niinemets, U. Responses of forest trees to single and multiple environmental stresses from seedlings to mature plants: Past stress history, stress interactions, tolerance and acclimation. *Forest Ecology and Management* **2010**, *260*, 1623 – 1639. doi:10.1016/j.foreco.2010.07.054.
65. Armas, C.; Padilla, F.M.; Pugnaire, F.I.; Jackson, R.B. Hydraulic lift and tolerance to salinity of semiarid species: consequences for species interactions. *Oecologia* **2010**, *162*, 11–21. doi:10.1007/s00442-009-1447-1.